The Astrophysical Journal Letters, 832:L20 (4pp), 2016 December 1 doi:10.3847/2041-8205/832/2/L20

MHD–KINETIC TRANSITION IN IMBALANCED ALFVÉNIC TURBULENCE

Yuriy Voitenko and Johan De Keyser
Solar-Terrestrial Centre of Excellence, BIRA-IASB, Ringlaan-3-Avenue Circulaire, B-1180 Brussels, Belgium
Received 2016 September 16; revised 2016 October 29; accepted 2016 November 7; published 2016 November 22

ABSTRACT

Alfvénic turbulence in space is usually imbalanced: amplitudes of waves propagating parallel and anti-parallel to the mean magnetic field $\boldsymbol{B}_0$ are unequal. It is commonly accepted that the turbulence is driven by (counter-) collisions between these counter-propagating wave fractions. Contrary to this, we found a new ion-scale dynamical range of the turbulence established by (co-)collisions among waves co-propagating in the same direction along $\boldsymbol{B}_0$. Co-collisions become stronger than counter-collisions and produce steep non-universal spectra above certain wavenumbers dependent on the imbalance. Spectral indexes of the strong turbulence vary around $\gtrsim -3$, such that steeper spectra follow larger imbalances. Intermittency steepens the -3 spectra further, up to -3.7. Our theoretical predictions are compatible with steep variable spectra observed in the solar wind at ion kinetic scales, but further verifications are needed by correlating observed spectra with measured imbalances.

Key words: solar wind – turbulence – waves

1. INTRODUCTION

Theory of strong Alfvénic turbulence (Goldreich & Sridhar 1995) predicts that the turbulence cascades anisotropically, mainly toward large perpendicular wavenumbers $k_\perp$ (small perpendicular scales $\lambda_\perp = 2\pi/k_\perp$) across the mean magnetic field, $\boldsymbol{k}_\perp \perp \boldsymbol{B}_0$. This prediction has been supported by observations of the solar-wind turbulence (MacBride & Smith 2008 and references therein). With growing $k_\perp$ the turbulent fluctuations become highly anisotropic, $k_\perp \gg k_z$ ($z \parallel \boldsymbol{B}_0$), and their perpendicular scales approach the ion gyroradius ρ_i. In this wavenumber range, MHD Alfvén waves (AWs) transform into kinetic Alfvén waves (KAWs; Hasegawa & Chen 1976).

Nonlinear KAW interactions differ significantly from nonlinear AW interactions and produce different turbulent spectra (Voitenko 1998a, 1998b; Schekochihin et al. 2009; Voitenko & De Keyser 2011; Boldyrev & Perez 2012 and references therein). Consequently, at certain sufficiently large wavenumber $k_\perp = k_{\perp *}$, the ion-scale spectral break should occur where the MHD AW turbulence transforms into the KAW turbulence. Recent observations of the solar-wind turbulence at ion kinetic scales support this scenario (He et al. 2012, Salem et al. 2012, Podesta 2013; Bruno et al. 2014; Roberts et al. 2015). KAW turbulence linked to MHD sources can develop also in solar (Zhao et al. 2013), terrestrial (Moya et al. 2015; Stawarz et al. 2015), and Jovian (von Papen et al. 2014) magnetospheres.

Theories of Alfvénic turbulence are relatively well developed in asymptotic MHD ($k_\perp^2\rho_i^2 \ll 1$) and kinetic ($k_\perp^2\rho_i^2 \gg 1$) ranges with perpendicular wavenumber spectra $\sim k_\perp^{-5/3}$ (or $\sim k_\perp^{-3/2}$) and $\sim k_\perp^{-7/3}$, respectively (Goldreich & Sridhar 1995; Gogoberidze 2007; Schekochihin et al. 2009 and references therein). The reference cross-field scale separating MHD and kinetic ranges is the ion gyroradius, $1/k_{\perp *} \sim \rho_i$, because finite-$k_\perp\rho_i$ effects distinguish KAWs from AWs. However, there is debate on the nature of ion-scale spectral break $k_{\perp *}$ and steep spectra at $k_\perp > k_{\perp *}$. Ion gyroradius ρ_i, ion inertial length δ_i, plasma β, turbulence amplitude B/B_0, turbulence anisotropy $k_{\perp *}/k_{z*}$, and several of their combinations have been suggested as relevant parameters fixing $k_{\perp *}$ (Markovskii et al. 2008; Chen et al. 2014; Boldyrev et al. 2015).

Solar-wind turbulence is imbalanced—amplitudes of waves propagating from the Sun $B_{k(+)}$ are usually larger than amplitudes of sunward waves $B_{k(-)}$, which can affect spectral transport (e.g., Beresniak & Lazarian 2008, Gogoberidze & Voitenko 2016; Yang et al. 2016 and references therein). A common theoretical assumption is that collisions between these counter-propagating AW fractions generate turbulence (Howes & Nielson 2013 and references therein). In this Letter, we show that collisions among co-propagating waves (co-collisions thereafter) at $k_{\perp *} < k_\perp < 1/\rho_i$ are stronger than counter-collisions and establish a new dynamical range of the turbulence. We shall refer to this as the weakly dispersive range (WDR). Similarly, we refer to the range $k_\perp\rho_i > 1$, where the kinetic modifications are strong, as the strongly dispersive range (SDR).

2. MODEL AND BASIC RELATIONS

Nonlinear dynamic equation for AW amplitudes, including both counter- and co-collisions of waves, has been derived by Voitenko (1998a). Here, we construct a semi-phenomenological model for the strong imbalanced Alfvénic turbulence from MHD to kinetic scales using the following approximation for the nonlinear interaction rate:

$$\gamma_{k\pm}^{\mathrm{NL}} = \frac{2+s}{4\pi} k_\perp V_A \Delta_{k,s} \frac{B_{k(\pm s)}}{B_0}, \qquad (1)$$

where the wave velocity mismatch $\delta V_{ks}/V_A \equiv \Delta_{k,s} = \sqrt{1+(k_\perp\rho_T)^2} - s$ and magnetic amplitude $B_{k(\pm s)} = B_{k\pm}$ for co-collisions ($s = 1$) and $B_{k(\pm s)} = B_{k\mp}$ for counter-collisions ($s = -1$). (1) is obtained from Equation (6.3) by Voitenko (1998a) assuming local interactions and separating dominant (+) and sub-dominant (−) waves propagating in opposite directions along $\boldsymbol{B}_0 \parallel \boldsymbol{z}$. Other definitions are: $\rho_T^2 \simeq (3/4 + T_{ez}/T_{i\perp})\rho_i^2$ at $k_\perp\rho_i < 1$ and $\rho_T^2 \simeq (1 + T_{ez}/T_{i\perp})\rho_i^2$ at $k_\perp\rho_i > 1$, T_{ez}—parallel electron temperature, $T_{i\perp}$—perpendicular ion temperature, $\rho_i = V_{Ti}/\Omega_i$—ion gyroradius, Ω_i—ion gyrofrequency,

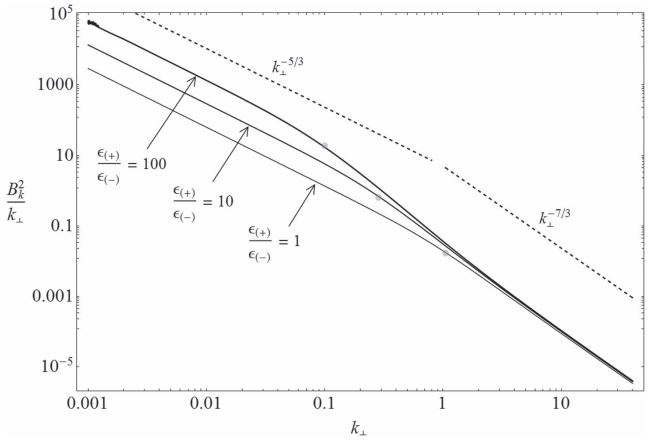

Figure 1. Spectra of the dominant (+) component of the strong Alfvénic turbulence (7) for different imbalance ratios $\epsilon_{(+)}/\epsilon_{(-)}$. Gray dots show breaks $k_{\perp *}$ calculated from (4). Perpendicular wavenumber $k_\perp$ is normalized by ρ_T; spectral powers are normalized to the same level in the SDR kinetic limit. Asymptotic MHD and SDR spectra $-5/3$ and $-7/3$ are shown for reference.

$V_{Ti} = \sqrt{T_{i\perp}/m_i}$—ion thermal velocity, and $V_A = B_0/\sqrt{4\pi n m_i}$—Alfvén velocity.

A simple phenomenological interpretation of (1) can be given in terms of colliding waves 1 and 2. The straining rate experienced by wave 1 in the magnetic shear of wave 2 is proportional not only to the shear $\lambda_\perp^{-1}(B_{k2}/B_0) \sim (2\pi)^{-1}k_\perp(B_{k2}/B_0)$, but also to the relative velocity $V_{\rm ph1} - sV_{\rm ph2}$ defining how fast the wave 1 moves across the shear. Product of these two factors, accounting for locality $k_{\perp 1} \sim k_{\perp 2} \sim k_\perp$ and KAW's dispersion $V_{\rm ph} = V_A\sqrt{1+(k_\perp\rho_T)^2}$ gives (1) within a factor of the order of one. The key element of (1) that distinguishes co- and counter-collisions is $\Delta_{k,s}$. Co-collisions ($s=1$) exist only for finite $k_\perp\rho_T \neq 0$, making $\Delta_{k,s} \neq 0$ and allowing co-propagating waves to move with respect to each other undergoing mutual straining. Counter-collisions ($s=-1$) operate throughout, $\Delta_{k,s} \geqslant 2$ for all $k_\perp\rho_T \geqslant 0$, as the counter-propagating waves pass through each other even if they are non-dispersive.

At $k_\perp\rho_T < 1$, (1) reduces to

$$\gamma_{k\pm}^{\rm NL(\uparrow\uparrow)} = \frac{1}{2\pi}(k_\perp\rho_T)^2 k_\perp V_A \frac{B_{k\pm}}{B_0}, \tag{2}$$

for co-collisions (superscript $\uparrow\uparrow$), and

$$\gamma_{k\pm}^{\rm NL(\uparrow\downarrow)} = \frac{1}{2\pi}k_\perp V_A \frac{B_{k\mp}}{B_0}. \tag{3}$$

for counter-collisions (superscript $\uparrow\downarrow$).

In the SDR, $k_\perp\rho_T > 1$, (1) gives

$$\gamma_{k+}^{\rm NL(\uparrow\downarrow)} \approx \frac{1}{3}\gamma_{k+}^{\rm NL(\uparrow\uparrow)} \approx \frac{1}{2\pi}(k_\perp\rho_T)k_\perp V_A\frac{B_{k-}}{B_0},$$

i.e., co-collisions and counter-collisions produce the same scalings.

3. MHD–KINETIC TRANSITION AND SPECTRA

In the asymptotic $k_\perp\rho_T \to 0$ MHD limit, $\gamma_{k\pm}^{\rm NL(\uparrow\uparrow)} \to 0$, and the turbulence is driven by counter-collisions, in compliance with Goldreih & Sridhar (1995) and many others. The cascade rate in the dominant component $\gamma_{k+}^{\rm TC(\uparrow\downarrow)} \sim (B_{k-}/B_{k+})^\mu\,\gamma_{k+}^{\rm NL(\uparrow\downarrow)}$, where $\mu = 0$, $1/2$, and 1 in the models by Lithwick et al. (2007), Beresniak & Lazarian (2008), and Chandran (2008), respectively. For all μ, the co-collision rate (2) increases with $k_\perp$ faster than $\gamma_{k+}^{\rm TC(\uparrow\downarrow)}$ and the transition occurs at

$$k_{\perp *}\rho_T \simeq \left(\frac{B_{k*(-)}}{B_{k*(+)}}\right)^{1/2+\mu}. \tag{4}$$

Above this wavenumber, the cascade is controlled by kinetic-type co-collisions.

The turbulence imbalance shifts $k_{\perp *}$ well below the $1/\rho_i$ opening window for a new dynamical range WDR $k_{\perp *} < k_\perp < 1/\rho_i$. In what follows, we consider the most unfavorable case $\mu = 0$ (Lithwick et al. 2007) with the largest $k_{\perp *}$ and narrowest WDR.

3.1. Scaling Relations

In the strong turbulence, energy fluxes $\epsilon_\pm = (\gamma_{k\pm}^{\rm NL(\uparrow\downarrow)} + \gamma_{k\pm}^{\rm NL(\uparrow\uparrow)})\,B_{k\pm}^2/(4\pi)$ can be presented as

$$\epsilon_\pm \approx \frac{B_0^2}{4\pi}\frac{k_\perp V_A}{4\pi}q_k\left(\frac{B_{k\mp}}{B_{k\pm}} + p_k\right)\left(\frac{B_{k\pm}}{B_0}\right)^3, \tag{5}$$

where $q_k = \Delta_{k,-1}$ and $p_k = 3\Delta_{k,1}/\Delta_{k,-1}$ are regular functions growing with $k_\perp$. Using (5) we express the fluxes ratio as

$$\frac{\epsilon_-}{\epsilon_+} = \frac{\left(1 + p_k\frac{B_{k-}}{B_{k+}}\right)}{\left(\frac{B_{k-}}{B_{k+}} + p_k\right)}\left(\frac{B_{k-}}{B_{k+}}\right)^2. \tag{6}$$

A real solution of this third-order equation for B_{k-}/B_{k+} is straightforward but too cumbersome to show explicitly. Denoting it by b_k, we find from (5) the amplitude scaling $B_{k+} \sim [k_\perp q_k(b_k + p_k)]^{-3}$ and spectrum

$$P_{k+} \equiv k_\perp^{-1}B_{k+}^2 \sim k_\perp^{-1}[k_\perp q_k(b_k+p_k)]^{-6}. \tag{7}$$

At $k_\perp\rho_T < 1$, to the leading order, $p_k \approx 0.75(k_\perp\rho_T)^2$, $q_k \approx 2$, and the amplitude ratio

$$\frac{B_{k-}}{B_{k+}} \equiv b_k \approx \frac{1}{2}\left(\frac{\epsilon_-}{\epsilon_+} + \sqrt{\left(\frac{\epsilon_-}{\epsilon_+} + 4(k_\perp\rho_T)^2\right)\frac{\epsilon_-}{\epsilon_+}}\right). \tag{8}$$

Depending on $4(k_\perp\rho_T)^2 \gtrless \epsilon_-/\epsilon_+$, the former "MHD" range $k_\perp\rho_T < 1$ splits into an asymptotic MHD range controlled by counter-collisions, and the kinetic WDR is controlled by co-collisions.

In the asymptotic MHD range $k_\perp\rho_T < 0.5\sqrt{\epsilon_-/\epsilon_+}$, the amplitude ratio (8) is $B_{k-}/B_{k+} \approx \epsilon_-/\epsilon_+$, and (5) gives the amplitude scaling $B_{k\pm} \sim k_\perp^{-1/3}$ and power spectrum $P_{k\pm} = k_\perp^{-1}B_{k\pm}^2 \sim k_\perp^{-5/3}$. These scalings reproduce those reported previously.

In WDR $0.5\sqrt{\epsilon_-/\epsilon_+} < k_\perp\rho_T < 1$, controlled by co-collisions, the amplitude ratio is $k_\perp$-dependent:

$$b_k \approx \sqrt{\frac{\epsilon_-}{\epsilon_+}}\,(k_\perp\rho_T). \tag{9}$$

Then, $B_{k+} \sim k_\perp^{-1}$ and spectrum

$$P_{k+} = k_\perp^{-1}B_{k+}^2 \sim k_\perp^{-3}. \tag{10}$$

Sub-dominant amplitudes $B_{k-} \sim$ const and $P_{k-} \sim k_\perp^{-1}$.

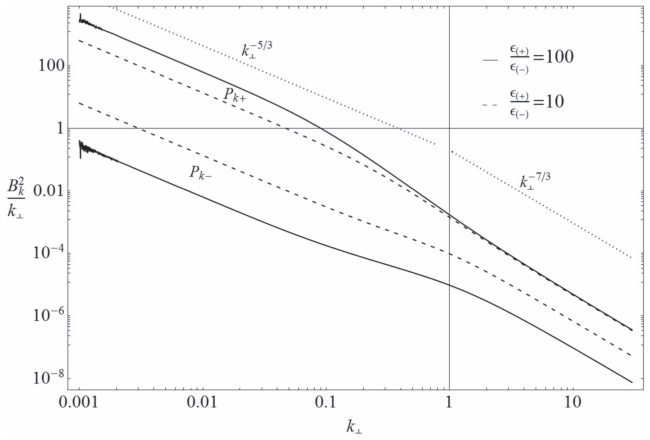

Figure 2. Spectra of the dominant (+) and sub-dominant (−) components of the strong turbulence for two imbalance ratios, $\epsilon_{(+)}/\epsilon_{(-)} = 10$ (dashed curves) and 100 (solid curves). The spectra converge stronger for a larger imbalance. Other notations as in Figure 1.

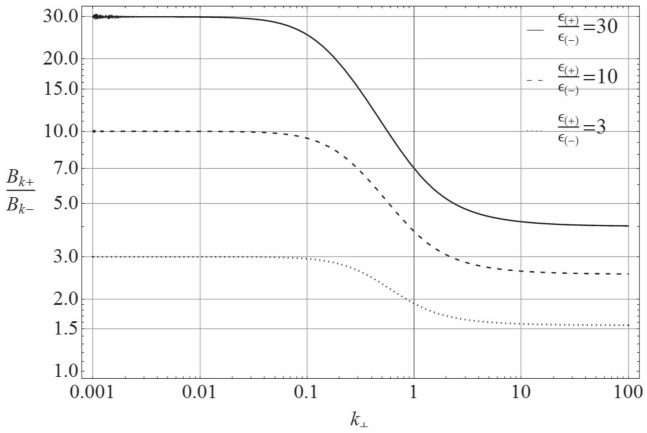

Figure 3. Ratio of (+)/(−) magnetic amplitudes for three imbalance ratios, $\epsilon_{(+)}/\epsilon_{(-)} = 30$, 10, and 3 from top to bottom. The amplitude ratio decreases significantly in the WDR.

In the SDR $k_\perp \rho_T > 1$, we have $p_k \approx 3$, $q_k \approx (k_\perp \rho_T)^2$, then $B_{k\pm} \sim k_\perp^{-2/3}$ and $P_{k\pm} \sim k_\perp^{-7/3}$ in both components.

Evolution of (+) waves in the WDR disconnects from (−) waves. As the linear decorrelation rate is $\gamma_k^{\mathrm{L}(\uparrow\uparrow)} \sim \omega_k^{\mathrm{dis}(\uparrow\uparrow)} \approx 0.5 k_z V_A (k_\perp \rho_T)^2$ (dispersive part of frequency), $k_{z+} \approx$ const follows from the critical balance condition $\gamma_k^{\mathrm{L}(\uparrow\uparrow)} \sim \gamma_k^{\mathrm{NL}(\uparrow\uparrow)}$. Evolution of parallel scales is thus suppressed in the WDR.

3.2. Non-universal Spectra

If the WDR is narrow (it is one order or less in the solar wind), the asymptotic spectrum $k_\perp^{-3}$ can hardly set up. Instead, variable spectra with indexes approaching -3 are expected in the WDR. This behavior is observed in Figure 1 where the spectra (7) are plotted without using asymptotic limits. The spectral indexes in the WDR vary $\gtrsim -3$, such that steeper spectra follow larger imbalances ϵ_+/ϵ_-.

Spectrum of − waves in the WDR is much shallower, $k_\perp^{-1}$, which leads to the convergence of + and − spectra. This effect is seen in Figure 2.

The imbalance of magnetic amplitudes is shown in Figure 3. The amplitude ratio decreases from $B_{k+}/B_{k-} = \epsilon_+/\epsilon_-$ in the asymptotic MHD range to $B_{k+}/B_{k-} = \sqrt{\epsilon_+/\epsilon_-}$ in the asymptotic kinetic range $k_\perp \gg \rho_i^{-1}$. The actual drop of the amplitude ratio is larger than the factor $\sqrt{\epsilon_+/\epsilon_-}$ because co-collisions are already partially operating before $k_{\perp *}$ and after ρ_i^{-1}. Say, if the original imbalance in the asymptotic MHD range is 30, then in the asymptotic kinetic range above $k_{\perp *}$ it drops to about 4, as is seen in Figure 3 (upper curve).

WDR spectra are affected by intermittency (Boldyrev & Perez 2012; Zhao et al. 2016). The modified spectra can be presented as $\tilde{P}_k \sim k_\perp^{-\alpha/3} P_k$, where $\alpha = 1$ for sheet-like and $\alpha = 2$ for tube-like fluctuations (Zhao et al. 2016). The WDR spectrum $P_k \sim k_\perp^{-3}$ thus steepens to $\tilde{P}_k \sim k_\perp^{-3.7}$, close to the steepest spectra reported by Leamon et al. (1999), Smith et al. (2006), and Sahraoui et al. (2010). Spectra $k_\perp^{-4}$ and even steeper can be formed in the weakly turbulent regime (Voitenko 1998b; Galtier & Meyrand 2015).

4. DISCUSSION

Some recent observations are compatible with the WDR triggered by imbalance. Bruno et al. (2014) and Bruno & Telloni (2015) have revealed that the ion-scale spectra are systematically steeper in the faster solar winds and suggested it may be caused by Alfvénicity, i.e., imbalance. Our theory supports this suggestion and explains why steeper spectra follow larger imbalances. Chen et al. (2014) have found that at low β the spectral breaks shift to scales larger than ρ_i and associated them with δ_i, which is hard to explain. We suggest that observed break scales can be related not to δ_i, but to $2\pi/k_{\perp *}$ defined by (4). The required imbalances $B_{k+}/B_{k-} = 2.1$and 3.1 in the models $\mu = 1$ and $1/2$ are realistic; $B_{k+}/B_{k-} = 9.8$ in the model $\mu = 0$ is less realistic. Observed spectral trends (see Figure 2(a) by Chen et al. 2014 and Figure 1(b) by Wicks et al. 2011) are the same as in our Figures 1 and 2 and agree with other WDR properties. Markovskii et al. (2007) argued that the break wavenumber decreases with increasing amplitude at break, which may be caused by the turbulence imbalance (it is usually larger at larger turbulence level). These observations are compatible with our theoretical predictions, but they did not measure imbalances to correlate with spectra. We are not aware of such observations so far.

Kinetic damping at ion scales has been widely discussed as a possible barrier for turbulent cascades (see, e.g., Leamon et al. 1999; Voitenko & Goossens 2004; Wu & Yang 2007; Podesta et al. 2010; Maneva et al. 2015; Cranmer 2014; Nariyuki et al. 2014; Passot & Sulem 2015). Nevertheless, nearly universal power-law turbulent spectra $k_\perp^{-2.8\pm0.3}$ are observed in the SDR up to electron gyroscales (Alexandrova et al. 2013 and references therein). Slight deviations from the theoretical spectra ($k_\perp^{-7/3}$ in strong and $k_\perp^{-2.5}$ in weak turbulence) can be attributed to intermittency (Boldyrev & Perez 2012) and damping (Passot & Sulem 2015). Actually, Zhao et al. (2016) argued that the damping modifies the spectral index by 0.1 only. This suggests that the damping is not so strong as thought before. In particular, quasi-linear diffusion reduces velocity-space gradients and wave damping (Voitenko & Goossens 2006; Pierrard & Voitenko 2013), which is supported by observations (He et al. (2015). We thus focused on nonlinear dynamics ignoring linear damping γ_k^{L}.

Non-universal spectra $k_\perp^{-2}$ to $k_\perp^{-4}$ observed at $k_\perp \lesssim 1/\rho_i$ (Leamon et al. 1999; Smith et al. 2006; Sahraoui et al. 2010)

are much steeper than the theoretical spectrum $k_\perp^{-5/3}$ formed by counter-collisions. Such strong steepening can hardly be caused by intermittency or damping without significant nonlinear modifications. Our theoretical results uphold the dominant role of nonlinear interactions at ion kinetic scales, where they are strengthened by co-collisions.

5. SUMMARY

We studied the MHD–kinetic transition in strong imbalanced Alfvénic turbulence and found a new dynamical range of the turbulence (WDR) at ion scales. Its main properties are:

1. The MHD–kinetic transition and spectral break in the imbalanced turbulence occur at $k_{\perp *}$ (4), above which the turbulence is controlled by kinetic-type co-collisions. For existing models of the imbalanced MHD turbulence ($\mu = 0; 1/2; 1$) the break $k_{\perp *}$ falls well below $1/\rho_i$ and a new dynamical range WDR arises at $k_{\perp *} < k_\perp < 1/\rho_i$.
2. Turbulent cascade is accelerated in the WDR and produces steep non-universal spectra. The spectral index varies from $\gtrsim -2$ to $\lesssim -4$ such that steeper spectra follow larger imbalances, stronger intermittency, or weak turbulence.
3. Magnetic amplitude ratio $B_{k(+)}/B_{k(-)}$ is not scale-invariant in the WDR decreasing from ϵ_+/ϵ_- to $\sqrt{\epsilon_+/\epsilon_-}$. Similarly, dominant and sub-dominant spectra converge in the WDR.
4. Evolution of the parallel wavenumber and frequency slows down in the WDR, and wavenumber anisotropy grows faster.

Models with $\mu > 0$ (Beresnyak & Lazarian 2008, Chandran 2008) reproduce the same spectra as in Figures 1–2 with significantly lower imbalances $B_{k(+)}/B_{k(-)}$ than those required in the $\mu = 0$ model (Lithwick et al. 2007). WDR spectra are steeper than in nearby MHD and SDR ranges, which results in a double-kink spectral pattern. This and other properties of the WDR are compatible with observations of the solar-wind turbulence at ion kinetic scales. Applicability of our theory to solar-wind turbulence needs further verification by correlating observed spectra with measured imbalances.

This research was supported by the Belgian Science Policy Office (through Prodex/Cluster PEA 90316 and IAP Programme project P7/08 CHARM).

REFERENCES

Alexandrova, O., Chen, C. H. K., Sorriso-Valvo, L., Horbury, T. S., & Bale, S. D. 2013, SSRv, 178, 101
Beresnyak, A., & Lazarian, A. 2008, ApJ, 682, 1070
Boldyrev, S., Chen, C. H. K., Xia, Q., & Zhdankin, V. 2015, ApJ, 806, 238
Boldyrev, S., & Perez, J. C. 2012, ApJL, 758, L44
Bruno, R., & Telloni, D. 2015, ApJL, 811, L17
Bruno, R., Trenchi, L., & Telloni, D. 2014, ApJL, 793, L15
Chandran, B. D. G. 2008, ApJ, 685, 646
Chen, C. H. K., Leung, L., Boldyrev, S., Maruca, B. A., & Bale, S. D. 2014, GeoRL, 41, 8081
Cranmer, S. R. 2014, ApJS, 213, 16
Galtier, S., & Meyrand, R. 2015, JPlPh, 81, 325810106
Gogoberidze, G. 2007, PhPl, 14, 022304
Gogoberidze, G., & Voitenko, Y. M. 2016, Ap&SS, 361, 364
Goldreich, P., & Sridhar, S. 1995, ApJ, 438, 763
Hasegawa, A., & Chen, L. 1976, PhFl, 19, 1924
He, J., Tu, C., Marsch, E., & Yao, S. 2012, ApJL, 745, L8
He, J., Wang, L., Tu, C., Marsch, E., & Zong, Q. 2015, ApJL, 800, L31
Howes, G. G., & Nielson, K. D. 2013, PhPl, 20, 072302
Leamon, R. J., Smith, C. W., Ness, N. F., & Wong, H. K. 1999, JGR, 104, 22331
Lithwick, Y., Goldreich, P., & Sridhar, S. 2007, ApJ, 655, 269
MacBride, B. T., & Smith, C. W. 2008, ApJ, 679, 1644
Maneva, Y. G., Vinas, A. F., Moya, P. S., Wicks, R. T., & Poedts, S. 2015, ApJ, 814, 33
Markovskii, S. A., Vasquez, B. J., & Smith, C. W. 2008, ApJ, 675, 1576
Moya, P. S., Pinto, V. A., Vinas, A. F., et al. 2015, JGRA, 120, 5504
Nariyuki, Y., Hada, T., & Tsubouchi, K. 2014, ApJ, 793, 138
Passot, T., & Sulem, P. L. 2015, ApJL, 812, L37
Pierrard, V., & Voitenko, Y. 2013, SoPh, 288, 355
Podesta, J. J. 2013, SoPh, 286, 529
Podesta, J. J., Borovsky, J. E., & Gary, S. P. 2010, ApJ, 712, 685
Roberts, O. W., Li, X., & Jeska, L. 2015, ApJ, 802, 2
Sahraoui, F., Goldstein, M. L., Belmont, G., Canu, P., & Rezeau, L. 2010, PhRvL, 105, 131101
Salem, C. S., Howes, G. G., Sundkvist, D., et al. 2012, ApJL, 745, L9
Schekochihin, A. A., Cowley, S. C., Dorland, W., et al. 2009, ApJS, 182, 310
Smith, C. W., Hamilton, K., Vasquez, B. J., & Leamon, R. J. 2006, ApJL, 645, L85
Stawarz, J. E., Ergun, R. E., & Goodrich, K. A. 2015, JGRA, 120, 1845
Voitenko, Y., & De Keyser, J. 2011, NPGeo, 18, 587
Voitenko, Y., & Goossens, M. 2004, NPGeo, 11, 535
Voitenko, Y., & Goossens, M. 2006, SSRv, 122, 255
Voitenko, Yu. M. 1998a, JPlPh, 60, 497
Voitenko, Yu. M. 1998b, JPlPh, 60, 515
von Papen, M., Saur, J., & Alexandrova, O. 2014, JGRA, 119, 2797
Wicks, R. T., Horbury, T. S., Chen, C. H. K., & Schekochihin, A. A. 2011, PhRvL, 106, 045001
Wu, D. J., & Yang, L. 2007, ApJ, 659, 1693
Yang, L., Lee, L. C., Chao, J. K., et al. 2016, ApJ, 817, 178
Zhao, J. S., Voitenko, Y. M., Wu, D. J., & Yu, M. Y. 2016, JGRA, 121, 5
Zhao, J. S., Wu, D. J., & Lu, J. Y. 2013, ApJ, 767, 109